Heterogeneous Leg Stiffness and Roll in Dynamic Running

Samuel Burden†, Jonathan Clark‡, Joel Weingarten‡, Haldun Komsuoglu‡, Daniel Koditschek‡
†Department of Electrical Engineering, University of Washington, Seattle, USA
‡Department of Electrical and Systems Engineering, University of Pennsylvania, Philadelphia, USA

***Abstract*— Legged robots are by nature strongly non-linear, high-dimensional systems whose full complexity permits neither tractable mathematical analysis nor comprehensive numerical study. In consequence, a growing body of literature interrogates simplified "template" [1], [2] models—to date almost exclusively confined to sagittal- or horizontal-plane motion—with the aim of gaining insight into the design or control of the far messier reality. In this paper we introduce a simple *bounding-in-place* ("BIP") model as a candidate frontal plane template for straight-ahead level ground running and explore its use in formulating hypotheses about whether and why rolling motion is important in legged locomotion. Numerical study of left-right compliance asymmetry in the BIP model suggests that compliance ratios yielding lowest steady state roll suffer far longer disturbance recovery transients than those promoting greater steady state roll. We offer preliminary experimental data obtained from video motion capture data of the frontal plane disturbance recovery patterns of a RHex-like hexapod suggesting a correspondence to the conclusions of the numerical study.**

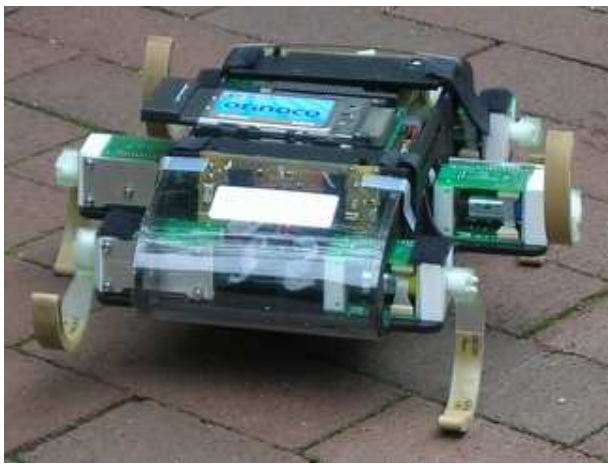

Fig. 1. EduBot [19], a RHex-like [20] hexapedal robot.

I. Introduction

As our understanding of the dynamics of running animals has increased, so has our ability to develop fast and stable running robots. Particularly important has been the development of the *Spring-Loaded Inverted Pendulum* (SLIP) model [3], [4], which captures the center of mass motions and ground reaction forces for a wide range of animals. Understanding how animal legs act like springs [5]—absorbing kinetic energy during touchdown and restoring it at liftoff—has encouraged [6] or led directly [7], [8] to the design of many dynamic runners. More recently, the development of the *Lateral-Leg Spring* (LLS) model [9], [10] has given insight into how the lateral forces exhibited by running animals can act to stabilize the lateral and yaw motions in the horizontal plane [11]. These models can be combined to suggest many salient features of legged locomotion dynamics.

In addition to oscillations in the sagittal and horizontal planes, animals and dynamic robots of various morphologies typically exhibit rolling motions not captured in either the SLIP or LLS model. The observation of a roll component in legged locomotion has a long history in robotics, stretching back at least two decades [12], and contemporary empirical research seems to confirm [13] the seeming inevitability of a substantial roll-pitch synchrony in legged trotting. More analytically inclined investigations of passive (downhill, gravitationally-driven) bipedal walking [14], [15] have shown that roll oscillation is unstable in spatial instances of these gaits [16]. Simple pelvic [17] or step-placement [16] feedback (the latter reminiscent of observed human gait control mechanisms [18]) can be shown to stabilize roll, but these "energetically natural" controllers do not seem to diminish its magnitude, notwithstanding the apparent energetic inefficiency it harbors through the exercise of seemingly inessential but inevitably lossy degrees of freedom. Beyond its seeming energetic inefficiency there are "higher level" objections to roll in steady state legged gaits. Such motion makes exteroceptive and even proprioceptive sensing more difficult. Visual data incurs a significant rotational overlay that necessitates extra processing; gyroscopic effects are harder to measure; and even tactile sensing by antennae or legs is complicated by alterations in touch-down timing arising from roll. From these perspectives, any design change that would reduce roll might seem to make the control of the robot more straightforward.

However, our intuition and experience with legged robotic systems leads us to an opposing hypothesis. In our previous work tuning RHex [21] and Sprawlita [22] it has always seemed that the best gaits incur significant roll dynamics. We suspect that these frontal plane oscillations actually confer significant dynamic benefit. In particular, we suspect that the attractors (hybrid limit cycles) associated with alternating tripod gaits in hexapedal runners have speedier restorative time constants in rough correspondence with the magnitude of their in-phase roll component.

In this paper we seek to investigate that hypothesis. To explore the effect of leg design on the frontal plane dynamics of running we introduce a candidate template - the *bounding-in-place* ("BIP") model. We explore numer-

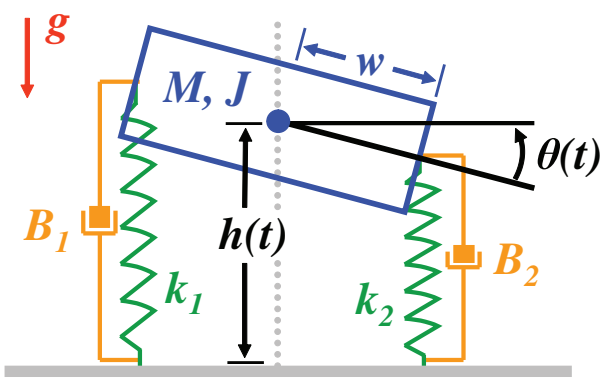

Fig. 2. *Bounding-in-place* ("BIP") model for legged rolling motion. In general, $k_1 \neq k_2$. We set $B_1 = B_2 = 0$ when we wish to study a conservative model.

ically the empirical fidelity of this model with respect to the EduBot [19]—a hexapedal RHex-like runner shown in Fig. 1. Like RHex [21], EduBot's reliance on an alternating tripod gait introduces an asymmetry to the frontal plane dynamics, since one side of the robot has two legs in contact with the ground, effectively doubling the stiffness of that side. Section II introduces the BIP model, and Section III describes a numerical study focused on the effect on roll stability of the relative stiffness between the alternating left- and right-weakened leg spring. Section IV describes the experimental setup and empirical consequences of varying the stiffness of the middle legs on Edubot. The model and experimental results are then compared and conclusions drawn in Section V.

II. Bounding-in-Place Model

We now introduce a hybrid dynamical system—the *bounding-in-place* ("BIP") model—intended to capture the salient aspects of EduBot's frontal-plane roll. Like the SLIP, LLS, and Buehler bounding models [23], we assume the robot's dynamics are decoupled and model roll independently of pitching, yawing, and translations along the ground plane. As in those prior simplified models, we combine several legs into a single *virtual leg*, in this case one on either side of the robot.

The BIP model consists of a rigid block with a Hooke's Law spring attached to either end. The center-of-mass is constrained laterally, thus allowing the body to move vertically and rotate about its center; it has width $2w$, mass M and moment of inertia J. The springs are oriented vertically and are allowed to slide frictionlessly across the ground; they have nominal length γ, spring constants k_1 and k_2, and damping constants B_1 and B_2, respectively (see Fig. 2)). The system proceeds through four distinct dynamical regimes: flight, left leg stance, right leg stance, and full stance.

EduBot runs using an *alternating tripod gait*, where the front and rear legs on one side of the robot cycle in phase with the middle leg on the opposite side. Due to the structural similarity between the legs, one side of the robot will have a virtual leg stiffness of effectively twice that of the other. We model the alternating aspect of the gait by exchanging the spring and damping constants—$(k_1, k_2, B_1, B_2) \mapsto (k_2, k_1, B_2, B_1)$—when the body transitions from full flight to partial stance.

The BIP model bears a striking schematic resemblance to Buehler's bounding model [23], but differs significantly in that Buehler's model allows the legs to rotate and the body to translate horizontally. As we will demonstrate, these differences are significant enough to eliminate the passive stability properties observed in the Buehler model.

A. Conservative BIP Model

Motivated by the discovery in the LLS model [9] and Buehler's bounding model [23] of stable open-loop gaits in a conservative model, we begin with no energy dissipation or addition in our model. We choose to describe the system's equations of motion in terms of the height of the block's center-of-mass h and its rotation θ. Straightforward analysis yields the governing equations,

$$\begin{aligned}\ddot{h}(t) &= \tfrac{1}{M}\Big[-gM + (\gamma - h(t))(\tilde{k}_1 + \tilde{k}_2) + \\ &\qquad w\sin(\theta(t))(\tilde{k}_1 - \tilde{k}_2)\Big], \\ \ddot{\theta}(t) &= -\tfrac{w}{J}\cos(\theta(t))\Big[(\gamma - h(t))(\tilde{k}_1 - \tilde{k}_2) + \\ &\qquad w\sin(\theta(t))(\tilde{k}_1 + \tilde{k}_2)\Big].\end{aligned} \tag{1}$$

where $\tilde{k}_i := \sigma_i k_i$ and σ_i is a Boolean variable set to 1 or 0 depending upon whether leg i is in stance or in flight.

Transitions between states are detected using *threshold equations*, which we'll describe using the *leg displacement coordinates* given by

$$x_1 = \gamma - (h - w\sin\theta), \;\; x_2 = \gamma - (h + w\sin\theta). \tag{2}$$

In particular, a necessary condition for a transition to occur is that a leg either touches down or leaves the ground,

$$x_1 = 0 \;\; or \;\; x_2 = 0. \tag{3}$$

When this condition is triggered, the pair (σ_1, σ_2) transitions according to certain functions of state. Specifically, let $z = (x_1, \dot{x}_1, x_2, \dot{x}_2)^T$ be the system state and let $\mathcal{H}_{(\sigma_1,\sigma_2)}(z)$ be the transition function out of the pair (σ_1, σ_2) so that when (3) is triggered, $(\sigma_1, \sigma_2) := \mathcal{H}_{(\sigma_1,\sigma_2)}(z)$.

$$\mathcal{H}_{(0,0)}(z) = \begin{cases} (1,1) & \text{if} \quad x_1 = 0,\ \dot{x}_1 \leq 0, \\ & \qquad x_2 = 0,\ \dot{x}_2 \leq 0; \\ (1,0) & \text{if} \quad x_1 = 0,\ \dot{x}_1 \leq 0, \\ & \qquad x_2 \neq 0 \ or \ \dot{x}_2 > 0; \\ (0,1) & \text{if} \quad x_1 \neq 0 \ or \ \dot{x}_1 > 0, \\ & \qquad x_2 = 0,\ \dot{x}_2 \leq 0; \\ (0,0) & \qquad \text{otherwise.} \end{cases} \tag{4}$$

$$\mathcal{H}_{(1,1)}(z) = \begin{cases} (0,0) & \text{if} \quad x_1 = 0,\ \dot{x}_1 > 0, \\ & \quad\ x_2 = 0,\ \dot{x}_2 > 0; \\ (1,0) & \text{if} \quad x_1 \neq 0 \ \textit{or}\ \dot{x}_1 \leq 0, \\ & \quad\ x_2 = 0,\ \dot{x}_2 > 0; \\ (0,1) & \text{if} \quad x_1 = 0,\ \dot{x}_1 > 0, \\ & \quad\ x_2 \neq 0 \ \textit{or}\ \dot{x}_2 \leq 0; \\ (1,1) & \quad\ \text{otherwise.} \end{cases}$$

$$\mathcal{H}_{(1,0)}(z) = \begin{cases} (0,1) & \text{if} \quad x_1 = 0,\ \dot{x}_1 > 0, \\ & \quad\ x_2 = 0,\ \dot{x}_2 \leq 0; \\ (0,0) & \text{if} \quad x_1 = 0,\ \dot{x}_1 > 0, \\ & \quad\ x_2 \neq 0 \ \textit{or}\ \dot{x}_2 > 0; \\ (1,1) & \text{if} \quad x_1 \neq 0 \ \textit{or}\ \dot{x}_1 \leq 0, \\ & \quad\ x_2 = 0,\ \dot{x}_2 \leq 0; \\ (1,0) & \quad\ \text{otherwise.} \end{cases}$$

$$\mathcal{H}_{(0,1)}(z) = \begin{cases} (1,0) & \text{if} \quad x_1 = 0,\ \dot{x}_1 \leq 0, \\ & \quad\ x_2 = 0,\ \dot{x}_2 > 0; \\ (0,0) & \text{if} \quad x_1 \neq 0 \ \textit{or}\ \dot{x}_1 > 0, \\ & \quad\ x_2 = 0,\ \dot{x}_2 > 0; \\ (1,1) & \text{if} \quad x_1 = 0,\ \dot{x}_1 \leq 0, \\ & \quad\ x_2 \neq 0 \ \textit{or}\ \dot{x}_2 \leq 0; \\ (1,0) & \quad\ \text{otherwise.} \end{cases}$$

Recall our statement that when the body transitions from full flight to partial stance its spring constants are exchanged; $(k_1, k_2) \mapsto (k_2, k_1)$. In terms of the transition functions defined above, this means the transitions $\mathcal{H}_{(0,0)} = (1,0)$ and $\mathcal{H}_{(0,0)} = (0,1)$ trigger the exchange.

An analytical account of this hybrid, tightly coupled, nonlinear dynamical model promises to be very complicated and lies well beyond the scope of the present paper. Instead, we turn to numerical simulations to study the system's behavior.

We used numerical simulations of the flow defined by (1), (3), and (4)) to generate system trajectories from a variety of initial conditions (see Appendices A, B). In particular, we searched for *equilibrium gaits* (defined as periodic orbits of the hybrid dynamical system defined by (1), (3), and (4)). We found several such gaits and chose to analyze the one that most closely mimics EduBot's. The EduBot-like gait has a full-flight phase and allows the derivative of the height to change sign only once during stance (i.e. the system's center-of-mass roughly traces out a sinusoid; see Fig. 4).

Using an iterative algorithm, we estimated the *touchdown state*—the body state when one leg touches down from flight—associated with the desired gaits to within one part in one million. We do this by computing the touchdown-to-touchdown Poincaré map $\mathcal{P}$ [24] at points with equal energy; periodic gates are determined by the fixed points of this map. Because the system is conservative, given h, θ, and one of $\dot{h}$ or $\dot{\theta}$, the other can be determined. Also, given either h or θ at touchdown, the other is determined by (3). Thus we need only search, for instance, over an interval in h-$\dot{h}$ space to estimate the locations of the fixed points of $\mathcal{P}$. At each step in our search algorithm, we compute the magnitude of

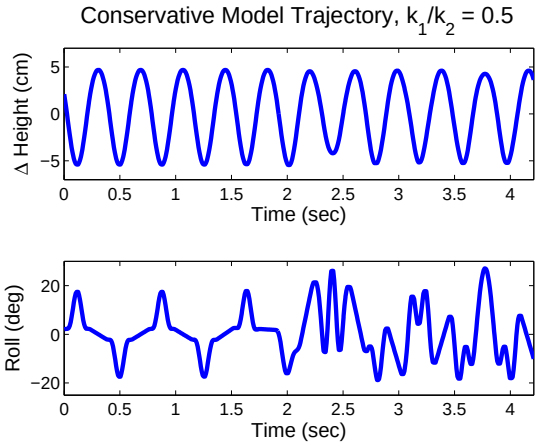

Fig. 3. Typical height and roll trajectory starting near an equilibrium gait in the conservative model. After only 6 strides, the body's rolling motion becomes extremely aperiodic, supporting the hypothesis that the conservative BIP model supports no stable equilibrium gaits.

$\mathcal{P}$ on a grid in some rectangular region of h-$\dot{h}$ space, then shrink the rectangle around the point $(\tilde{h}^*, \tilde{\dot{h}}^*)$ corresponding to the smallest value of $|\mathcal{P}(z) - z|$. Assuming there is only one fixed point of $\mathcal{P}$ in the initial region, this algorithm will estimate the touchdown state of the desired equilibrium gaits to arbitrary precision.

No matter how stringent our error tolerances, however, we always found these gaits to be unstable, as Fig. 3 illustrates. This is interesting because it is not *a priori* unreasonable to imagine that the conservative model's hybrid dynamics could have generated an asymptotically stable gait (as occurs in the LLS and Buehler models). However, given that errors on the order of 1×10^{-6} in the touchdown state estimate cause large trajectory deviations after only a few strides, we consider this a poor model to study stability properties of EduBot's gait, and introduce damping to try to capture the robot's stable periodic behavior.

B. Dissipative BIP Model

In an effort to make the equilibrium gaits of this model attracting, and to better approximate the physical system, we add viscous damping to the conservative model, so that the equations of motion include a term proportional to the negative of the velocity of the point of attachment of each spring. The constants of proportionality are the *damping constants* B_1 and B_2, which we fix at $k_2/70$, smaller than that measured in EduBot's legs. Even using this rough approximation to the complex physical interactions that drive EduBot's motion, we observe qualitative agreement between body trajectories in the model and EduBot trajectories (see Fig. 4).

Since energy is continually removed from the system with the addition of damping, we restore the possibility of a periodic trajectory by adding energy to the system in a manner similar to that employed by Koditschek and Buehler [25] in analyzing one-dimensional hopping. When a leg spring reaches maximum compression in the model, we temporarily

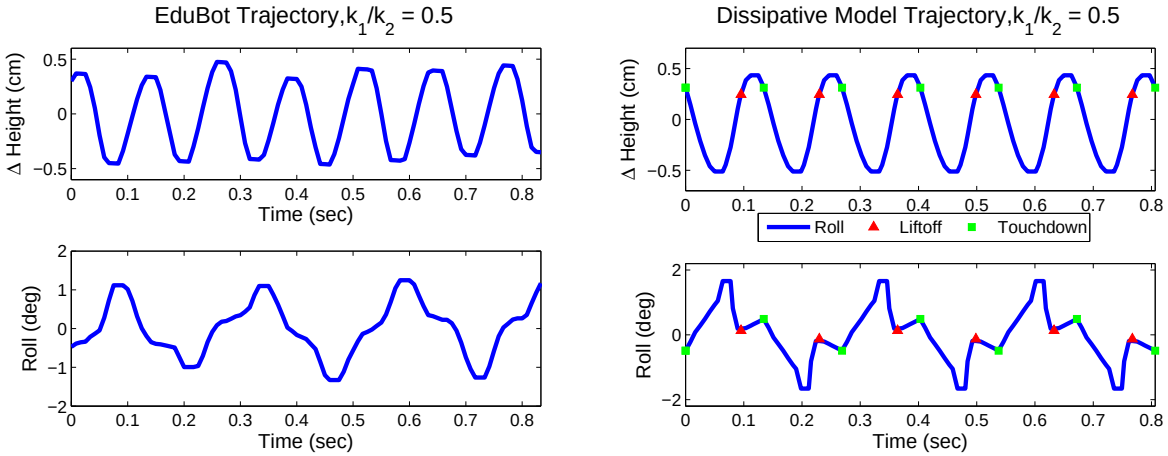

Fig. 4. Typical height and roll trajectories from EduBot and from the dissipative model. Both data sets were sampled at 120 Hz and filtered with a 5-sample median filter as described in Section IV. The model deviates in magnitude and precise shape in both coordinates, but qualitatively captures some of the distinctive behavior exhibited by the robot. We attribute the difference in the shape of the roll trajectories largely to EduBot achieving a smaller flight phase than the model.

increase its spring constant, thus increasing the energy stored in the spring. This actuation scheme was chosen because it is easy to implement and can facilitate analysis better than many other methods. Maximum compression is detected when a leg's velocity goes to zero from below,

$$\dot{x}_1 \uparrow 0 \ or \ \dot{x}_2 \uparrow 0. \tag{5}$$

At that instant, the leg's spring constant is increased by a factor $\eta > 0$ chosen to yield gaits qualitatively similar to the physical robot. When a leg leaves the ground in simulation, its spring constant is reset to its initial value.

For the case of our tripod-based runner we increase η twice as much for the stiffer (double support) leg, reflecting our observation that in the physical system each of EduBot's legs imparts a roughly equal vertical force on the ground during stance. This observation is consistent with the biological literature [26], and is qualitatively corroborated by the profile of the vertical ground reaction forces exerted on EduBot's front, rear, and middle legs (see Fig. 5).

As we demonstrate in the next section, adding damping to the model indeed produces the expected stable equilibrium gaits (isolated period-one attracting orbits). This removes the necessity to use an iterative method when searching for periodic orbits, since we can simply allow the simulation to settle into equilibrium and record the touchdown state at that point.

III. Design Modifications and Stability

Having established our model for rolling dynamics, we proceed to investigate modifications that eliminate roll and the effect of these modifications on the stability of equilibrium gaits. Our model was designed assuming that roll is introduced primarily by a difference in effective leg stiffness between the two sides of EduBot. Thus we investigate the effect that stiffening the softer leg has on roll. In the model, we fix k_2, start with $k_1/k_2 = 0.25$, and increase that ratio

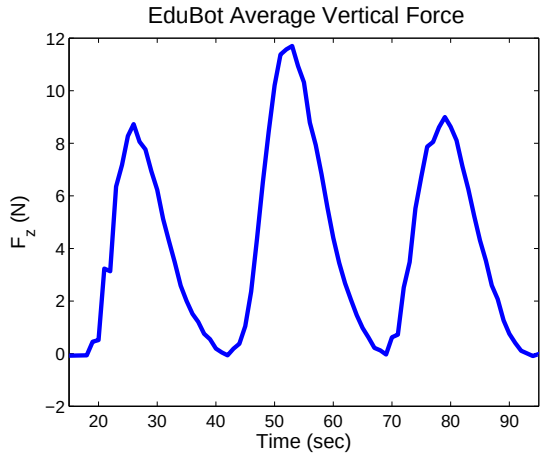

Fig. 5. Vertical ground reaction force profile for EduBot's left side. Measured with a commercial force plate [27], sampled at 200 Hz, averaged over 12 trials.

to 1. In the physical system, we affix middle legs of varying stiffness to the robot.

Fig. 6 displays the roll and its velocity at touchdown for the equilibrium gait associated with different values of k_1 when all other parameters are held fixed ($k_2 = 1440$ N/m). Because there is no energy loss in flight the roll velocity at touchdown is a reasonable measure of the roll velocity magnitude averaged over an entire orbit. Hence, the plot suggests that roll magnitude at touchdown is a surrogate for the intensity of the rolling associated with a given equilibrium gait. As $k_1/k_2 \to 1$, both roll and its velocity at touchdown increase monotonically, passing near the origin at $k_1/k_2 \approx 0.7$ ($k_1 \approx 1010$ N/m). Thus the model predicts that as EduBot's middle legs are made stiffer, the robot's roll magnitude will decrease until the ratio of stiffnesses is near $\frac{7}{10}$, then increase as the ratio increases to

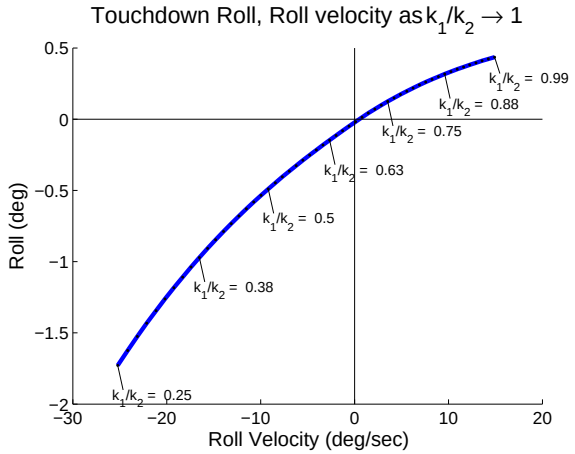

Fig. 6. Body roll and its velocity at touchdown as $k_1/k_2 \rightarrow 1$. This plot suggests that the roll magnitude at touchdown is a reasonable surrogate for the intensity of the rolling associated with a given equilibrium gait.

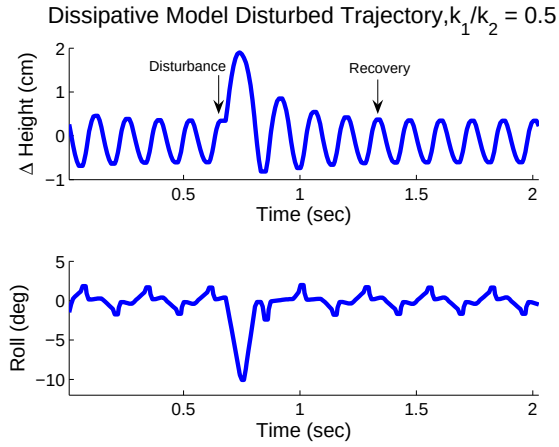

Fig. 7. Simulation results: trace of the dissipative model height and roll variables over time taken from a typical disturbance run.

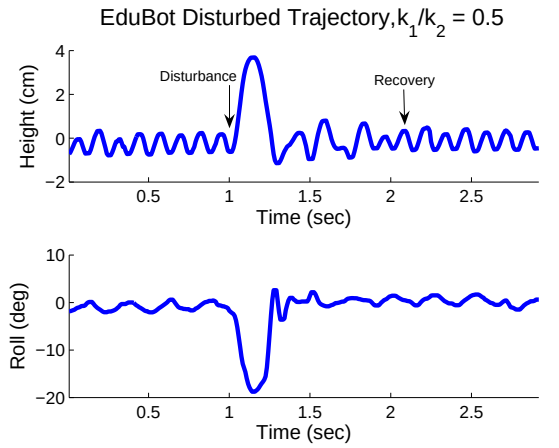

Fig. 8. Experimental results: trace of the physical robot's body height and roll variables over time taken from a typical disturbance run.

unity[1].

A. Stability Prediction

Based on our experience with EduBot and RHex, we hypothesize that increasing $k_1/k_2 \rightarrow 1$ makes the robot's gait less dynamically stable. We investigate the effect of this parametric change on stability in two ways: first, we test the time to recover from a disturbance; second, we numerically compute the Jacobian of the touchdown-to-touchdown Poincaré map [24] and use the magnitude of the eigenvalues of this matrix as a stability metric, as in [23], [28].

1) Disturbance Response: We allow the body to settle into an equilibrium gait, then disturb it by applying an instantaneous vertical force and angular torque at touchdown; this is qualitatively similar to the disturbance applied experimentally (see Section IV-C) and produces qualitatively similar response trajectories (see Figs. 7 and 8), though we do not have a quantitative comparison. We record the *disturbance recovery time* as the time between the disturbance and the next *stable touchdown*. When the body touched down on its left leg spring, its vertical velocity was increased by 0.75 m/sec and its roll velocity was decreased by 3 rad/sec. We define a stable touchdown as having the property that the average touchdown state over the subsequent five half-strides is within 0.3% of the equilibrium touchdown state. We then compare these responses for different choices of k_1 by plotting recovery time against the ratio k_1/k_2. Fig. 7 shows an example disturbed trajectory.

Fig. 9 shows the results of the disturbance study. As can be seen in the figure, recovery time reaches a minimum around $k_1/k_2 \approx 0.5$, with a large spike near $k_1/k_2 \approx 0.7$. Thus the model predicts that as EduBot's middle leg is made stiffer, it will become less dynamically stable until k_1/k_2 exceeds ≈ 0.7, at which point the stability will increase again, though the gait will still be less stable than it was when $k_1/k_2 \approx 0.5$.

2) Numerical Jacobian: As another estimate of the stability of equilibrium gaits, we numerically compute the Jacobian of the numerically integrated touchdown-to-touchdown map $\mathcal{P}$ at its fixed point z^* (which corresponds to an equilibrium gait) and compute the magnitude of the eigenvalues of this matrix.

We compute the Jacobian using the following method. First, we identify a fixed point z^* to within a desired tolerance ϵ in each coordinate; here $\epsilon \leq 1 \times 10^{-8}$. Then we compute the system's trajectory for a half-stride starting from two points $z^*_{+\delta_j}$, $z^*_{-\delta_j}$ a small displacement $1 \gg \delta_j \gg \epsilon$ ahead of and behind the fixed point in the j^{th} coordinate. We then estimate the partial derivative of the stride map with respect to the j^{th} component as

[1]Note the zero crossing occurs well before $k_1/k_2 = 1$ since with evenly balanced legs, the relevant periodic gait (associated with zero roll) is unstable in consequence of our simplified energy restoration model. The legs would have to repeatedly achieve maximum compression at precisely the same moment in order to preserve the gait—clearly unsupportable at steady state for numerical as well as dynamical reasons.

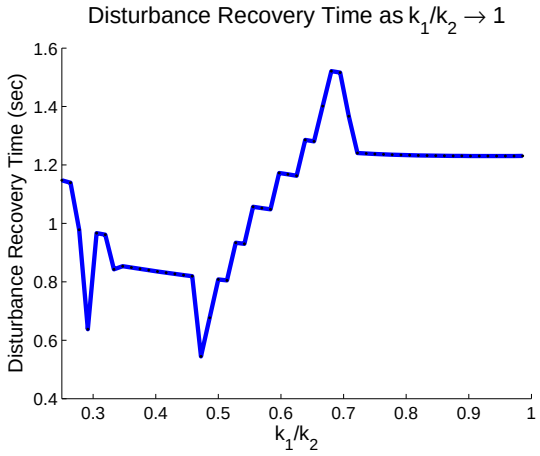

Fig. 9. Time required for simulated body to fluctuate less than 0.3% from the equilibrium gait as $k_1/k_2 \to 1$ after the disturbance $(\dot{h}, \dot{\theta}) \mapsto (\dot{h}+0.75$ m/sec, $\dot{\theta}-3$ rad/sec$)$. Discrete jumps occur because we only test for recovery at touchdown.

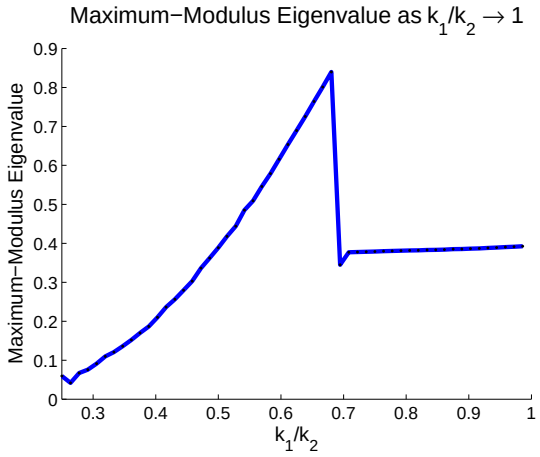

Fig. 10. Maximum-modulus eigenvalue of the Jacobian matrix of the touchdown-to-touchdown Poincaré map as $k_1/k_2 \to 1$. Discontinuity occurs when the touchdown state moves from the third quadrant to the first quadrant in Fig. 6. $\delta_{\dot{h}} = 0.01$, $\delta_\theta = 0.001$, $\delta_{\dot{\theta}} = 0.02$.

$$\Delta_j = \frac{\mathcal{P}(z^*_{+\delta_j}) - \mathcal{P}(z^*_{-\delta_j})}{2\delta_j} \tag{6}$$

and form the (4×4) Jacobian matrix

$$\Delta_{\mathcal{P}} = \begin{bmatrix} \Delta_h & \Delta_{\dot{h}} & \Delta_\theta & \Delta_{\dot{\theta}} \end{bmatrix}. \tag{7}$$

Because the return map is defined over a three dimensional "section"—specifically, h and θ are related algebraically at touchdown by (3)—we do not look at the eigenvalues of the full Jacobian matrix, and instead work with the (3×3) submatrix that excludes the row and column associated with the "dependent" variable, h.

Fig. 10 shows the result of this computation. This plot corroborates roughly the corresponding account in Fig. 9, strengthening the hypothesis that the model predicts a reduced quality of dynamic stability as $k_1/k_2 \to 0.7$, followed by a small increase in stability in the range $0.7 < k_1/k_2 < 1$. The apparent discontinuity in this figure occurs at the same value of k_1/k_2 as caused the the touchdown state to cross the origin in Fig. 6. This discontinuity is explained by the fact that the two sides of the origin correspond to two qualitatively different gaits in simulation.

3) Summary: By adding viscous damping to the conservative model of Section II-A, equilibrium gaits in the system become stable. By increasing the ratio k_1/k_2 in the dissipative model, the body's roll decreases to nearly zero at $k_1/k_2 \approx 0.7$, but increases as that ratio is increased further. In addition, as $k_1/k_2 \to 1$ from 0.5, gait stability decreases significantly, and this result was demonstrated using two different stability metrics. The fact that the minimum touchdown roll doesn't occur when $k_1/k_2 \approx 1$ seems to be an artifact of our energy addition scheme, and may not appear when other schemes are used.

IV. Experimental Results

In order to evaluate the dissipative model's relevance to the robot and to check whether the relationship between the magnitude of the roll and the stability of the rolling motions holds for the robot, we perform experiments to investigate the effect increasing k_1/k_2 has on EduBot's gait. Specifically, we collect trajectory data to compute the average rotational displacement as well as EduBot's disturbance response as k_1 is increased.

A. Experimental Methods

Our experimental platform is EduBot [19], a RHex-like hexapedal robot. EduBot measures approximately 30 cm long and 11 cm wide, its legs are 8 cm long, and its mass is approximately 1.4 kg. Similarly to RHex, EduBot's legs are semicirular and revolve about their hips and the robot employs an *alternating-tripod gait*, where the front and back legs on one side of the robot cycle in phase with the middle leg on the other side. In contrast to RHex, EduBot's legs are made from polyurethane resins, affording easy experimentation with a variety of leg stiffnesses. We tune the robot's gait by adjusting a variety of parameters as in [21], and use the same gait parameters for all experiments. The particular gait we selected has a *duty cycle* of less than 50%, meaning all the robot's legs leave the ground for a short time during a stride. We call this a *jogging gait*.

Trajectory measurements for the robot were recorded with a video-based motion capture system that uses Vicon 6 strobed cameras. The system treats EduBot as a rigid body in $\mathbb{R}^3$, recording the robot's position and rotation along three axes at approximately 120 Hz with sub-millimeter accuracy. Occasionally the motion capture system loses track of the robot for up to five samples; in this case, we interpolate linearly across the lost samples. We then apply a 5-sample median filter to smooth jump discontinuities in the data that appear to be introduced by noise. This filter has the effect of rounding cusps in the roll trajectory data, but otherwise alters the data minimally.

TABLE I

EDUBOT ROLL DISPLACEMENT, THREE MIDDLE LEG STIFFNESSES.

k_2	k_1 (N/m)	Maximum roll (deg)	# of Strides
1454	604	4.1 ± 0.4	42
1454	727	2.5 ± 0.6	42
1454	851	1.9 ± 0.5	68

TABLE II

EDUBOT DISTURBANCE RESPONSE, TWO MIDDLE LEG STIFFNESSES.

k_2	k_1 (N/m)	# of strides to recovery	# of experiments
1454	727	4.5 ± 0.9	8
1454	851	5.75 ± 0.5	8

B. Gait Trajectory

We allowed the robot to settle into an equilibrium jogging gait over 6-20 strides and recorded its trajectory using the motion capture system described above. We then extracted the roll trajectory data and computed the average roll displacement over several experiments. Table I shows that the average roll decreases by 50% from 4.1 to 1.9 degrees as $k_1 \rightarrow k_2$.

C. Disturbance Response

We disturb the robot in a manner similar to simulation. First, EduBot runs across a four-foot-long platform until it achieves an equilibrium jogging gait. Then, when it crosses the middle of a platform, we manually actuate a see-saw platform segment, lifting and retracting the platform under one side of EduBot several centimeters in approximately a half a second, imparting a vertical force and angular torque; Fig. 8 presents the sample traces of body height and roll recorded during a typical disturbance experiment. Since EduBot's trajectory is not as consistant as that of the simulation, a coarser stability metric is required. Specifically, we use the period of EduBot's gait as a discrete unit of time and count the number of full leg cycle periods required for the robot to return to an equilibrium gait; we identify equilibrium gaits visually.

We performed two sets of these disturbance experiments, one with $k_1/k_2 \approx \frac{1}{2}$ and the other with $k_1/k_2 \approx \frac{6}{10}$. The results are summarized in Table II. As can be seen in that table, our preliminary results suggest that disturbance response time increases as the fraction k_1/k_2 is increased from $\frac{5}{10}$ to $\frac{6}{10}$, which is consistent with the result from the model.

V. DISCUSSION

In this paper we have begun to explore the function of roll in dynamic legged locomotion. We have hypothesized that oscillatory roll motion will prove to play a significant role in the overall stability of the system. We have developed a novel, greatly simplified, hence, tractable model of the roll component in a running hexapod. Numerical results from this model match reasonably closely preliminary experiments on our physical robotic platforms, that demonstrated the strong effect of varied relative leg stiffness on the characteristic roll dynamics. More interestingly, the simulations corroborate (and the few preliminary experiments do not contradict) our hypothesis that as the magnitude of the periodic roll motion goes to zero, the system's ability to reject disturbances is reduced.

As stated, the results of experimentation on the physical system are preliminary. In particular, more systematic empirical work may reveal that the very simple energy restoration strategy introduced in this model may diminish the quality of more symmetrically sprung roll oscillations as an artifact of simulation along the lines of the observation in footnote 1. In the near future we will conduct more exhaustive experimentation on our systems to further probe the central hypothesis. We will examine the correlation between reduced roll and the energy efficiency and other dynamics of the system as well as the system's ability to traverse rough or broken terrain as roll dynamics are altered. Finally, we hope to work with biologists to verify these results on biological systems.

ACKNOWLEDGMENTS

We would like to thank Sam Russem for his help with the experiments and his construction of the variable-stiffness legs. In addition, we thank Philip Holmes and Manoj Srinivasan for helpful comments on the presentation and relevant background literature. Jonathan Clark was supported by the IC Postdoctoral Fellow Program under grant number HM158204-1-2030. Samuel Burden was supported by the SUNFEST REU program at the University of Pennsylvania. This work was also partially supported by the NSF FIBR grant #0425878.

APPENDIX

A. Model Parameters

The model parameters were chosen to approximate those of Edubot, with: $w = 10.75$ cm, $M = 1.2$ kg, $J = \frac{1}{6}Mw^2$ kg m^2, $\gamma = 8$ cm, $k_2 = 1440$ N/m, k_1 varies between 360 and 1420 N/m, $B_1 = B_2 = k_2/70$, and $\eta = 2500$ N/m; these values roughly match the robot's, though the moment of inertia is computed as if EduBot were a uniform rod and η is chosen to make the model behave qualitatively similar to the robot.

B. Numerical Methods

We use the Matlab `ode45` solver to compute the flow of (1) that advances the state until a transition event (3) is flagged by the Matlab root solver [29]. The transition function (4) is then applied and we return to the computation of (1).

REFERENCES

[1] R. J. Full and D. E. Koditschek. Templates and anchors: Neuromechanical hypotheses of legged locomotion on land. *Journal of Experimental Biology*, 202(23):3325–3332, 1999.

[2] R. Ghigliazza, R. Altendorfer, P. Holmes, and D. Koditschek. A simply stabilized running model. *SIAM Review*, 47(3):519–550, 2005.

[3] G. A. Cavagna, N. C. Heglund, and Taylor C. R. Mechanical work in terrestrial locomotion: Two basic mechanisms for minimizing energy expenditure. *American Journal of Physiology*, 233, 1977.

[4] R. Blickhan and R. J. Full. Similarity in multilegged locomotion: Bounding like a monopod. *Journal of Comparative Physiology*, 173(5):509–517, 1993.

[5] R.M. Alexander. Three uses for springs in legged locomotion. *International Journal of Robotics Research*, 9(2):53–61, 1990.

[6] Marc H. Raibert. *Legged robots that balance*. MIT Press series in artificial intelligence. MIT Press, Cambridge, Mass., 1986.

[7] R. Altendorfer, N. Moore, H. Komsuoglu, M. Buehler, Jr. Brown H. B, D. McMordie, U. Saranli, R. Full, and D. E. Koditschek. Rhex: A biologically inspired hexapod runner. *Autonomous Robots*, 11(3):207–213, 2001.

[8] J. G. Cham, J. Karpick, J. E. Clark, and M. R. Cutkosky. Stride period adaptation for a biomimetic running hexapod. In *International Symposium of Robotics Research*, Lorne Victoria, Australia, 2001.

[9] J. Schmitt and P. Holmes. Mechanical models for insect locomotion: Dynamics and stability in the horizontal plane i. theory. *Biological Cybernetics*, 83(6):501–515, 2000.

[10] J Schmitt, M Garcia, RC Razo, P Holmes, and RJ Full. Dynamics and stability of legged locomotion in the horizontal plane: a test case using insects. *Biological Cybernetics*, 86(5):343–53, 2002.

[11] T.M. Kubow and R.J. Full. The role of the mechanical system in control: a hypothesis of self-stabilization in hexapedal runners. *Philos. Trans. R. Soc. Lond.*, 354(1385):849–861, 1999.

[12] J. Glower and U. Ozguner. Control of a quadruped trot. In *Proceedings. 1986 IEEE International Conference on Robotics and Automation*, 1986.

[13] H. Kimura, Y. Fukuoka, and T. Mimura. Dynamics based integration of motion adaptation for a quadruped robot "tekken". In *Proceedings of the 2nd International Symposium on Adaptive motion of Animals and Machines*, 2003.

[14] T. McGeer. Passive dynamic walking. *International Journal of Robotics Research*, 9(2):62–82, 1990.

[15] S. H. Collins, M. Wisse, and A. Ruina. A three-dimensional passive-dynamic walking robot with two legs and knees. *The International Journal of Robotics Research*, 20(7):607–615, 2001.

[16] A. D. Kuo. Stabilization of lateral motion in passive dynamic walking. *IJRR*, 18:917–930, 1999.

[17] M. Wisse, A. L. Schwab, and Linde R. Q. vd. A 3d passive dynamic biped with yaw and roll compensation. *Robotica*, 19:275–284, 2001.

[18] C. E. Bauby and A. D. Kuo. Active control of lateral balance in human walking. *Journal of Biomechanics*, 33:1433–1440, 2000.

[19] H. Komsuoglu. Towards a comprehensive infrastructure for construction of modular and extensible robotic systems. Technical report, Department of Computer and Information Science, University of Pennsylvania, 2007.

[20] U. Saranli, M. Buehler, and D. Koditschek. Rhex: A simple and highly mobile hexapod robot. *The International Journal of Robotics Research*, 20(7):616–631, July 2001.

[21] J. Weingarten, G. Lopes, M. Buehler, R. Groff, and D. Koditschek. Automated gait adaptation for legged robots. volume 3, pages 2153–2158. International Conference on Robotics and Automation, 2004.

[22] J. E. Clark and M. R. Cutkosky. The effect of leg specialization in a biomimetic hexapedal running robot. *Journal of Dynamic Systems, Measurement, and Control*, 2006.

[23] I. Poulakakis, E. Papadopoulos, and M. Buehler. On the stable passive dynamics of quadrupedal running. International Conference on Robotics & Automation, September 2003.

[24] J. Guckenheimer and P. Holmes. *Nonlinear Oscillations, Dynamical Systems, and Bifurcations of Vector Fields*. Number 42 in American Mathematical Sciences. Springer-Verlag, New York, 2002.

[25] M. Buehler and D. Koditschek. Analysis of a simplified hopping robot. *International Journal of Robotics Research*, 10(6):587–605, 1991.

[26] R. Full and M. Tu. Mechanics of a rapid running insect: Two-, four-, and six-legged locomotion. *Journal of Experimental Biology*, 156:215–231, 1991.

[27] Advanced Mechanical Technology Inc. He6x6 force plate. 2006. http://www.amtiweb.com/index.htm.

[28] J. Cham and M. Cutkosky. Adapting work through actuator phasing. International Symposium on Adaptive Motion of Animals and Machines, March 2003.

[29] L. F. Shampine and M. W. Reichelt. The matlab ode suite. *SIAM Journal on Scientific Computing*, Vol. 18:1–22, 1997.